

## ULTRAVIOLET AND VISUAL WAVELENGTH SPECTROSCOPY OF GAS AROUND ETA CARINAE

KRIS DAVIDSON<sup>1,2</sup>

University of Minnesota

REGINALD J. DUFOUR<sup>2</sup>

Rice University

NOLAN R. WALBORN

Space Telescope Science Institute

AND

THEODORE R. GULL

NASA/Goddard Space Flight Center

Received 1985 September 23; accepted 1985 December 6

### ABSTRACT

We report observational results on  $\eta$  Carinae, especially spectroscopy of the outer "S condensation" supplemented by data on the homunculus and its core. Theoretical calculations of atmosphere/wind models and of the shock-heated S condensation are needed for a proper analysis of our data, but we discuss some simplified results. The helium abundance at the surface of  $\eta$  Car appears to be roughly  $Y \approx 0.4$ , and most of the CNO is nitrogen. There does not appear to be any reason, at present, to alter the often quoted temperature estimate  $T \approx 30,000$  K for the radiating surface (which may or may not be the surface of the star itself). The presently observed mass loss rate is probably less than  $10^{-2.4} M_{\odot} \text{ yr}^{-1}$  if the outflow is not strongly direction-dependent. Finally, we mention a largely forgotten but highly relevant historical conjecture concerning  $\eta$  Car.

*Subject headings:* nebulae: individual — stars: abundances — stars: massive — ultraviolet: spectra

### I. INTRODUCTION

The significance of  $\eta$  Carinae remained highly conjectural, despite its fame, until the 1970s. Since then it has become one of our most definite clues to the fate of very massive stars—provided, of course, that our "most likely" interpretation of its nature is valid. This star's colossal outburst observed around 1840 and its subsequent apparent behavior have been recounted many times; see Walborn and Liller (1977), de Jager (1980), van Genderen and Thé (1985), and references therein. Before 1970, many astronomers suspected that  $\eta$  Car had undergone a supernova event of some unfamiliar type. However, infrared observations by Westphal and Neugebauer (1969) showed that its luminosity continues almost unabated at a value of the order of  $10^{6.6} L_{\odot}$ . Ultraviolet and visual-wavelength radiation from the star is mostly absorbed by dust that has formed in the ejecta from the great 19th century explosion, and this dust-absorbed luminosity is reradiated at infrared wavelengths. After the infrared discovery, various arguments suggested that the star's basic spectrum emerges at a temperature around 30,000 K from an opaque surface which may or may not be the true stellar surface (Davidson 1971). At about the same time, luminous O3-type stars were discovered in association with  $\eta$  Car (Walborn 1971, 1973). As a working hypothesis, therefore,  $\eta$  Car is a very massive star like one of the most luminous O3 stars (its initial mass was probably at least  $150 M_{\odot}$ , befitting its luminosity), but cooler than the O3 stars, either because

it is a pre-main-sequence object or else because it is more evolved than the O3 stars. The discovery that its ejecta have been processed in the CNO cycle (Davidson, Walborn, and Gull 1982) showed that the star is evolved and is not pre-main-sequence. The same discovery also provided the simplest, most incisive proof that widespread mixing occurs in a moderately evolved, very massive star.

Eta Car seems to be at the upper limit allowed for stars in the Hertzsprung-Russell diagram. As a star whose initial mass exceeds  $60 M_{\odot}$  evolves, its surface becomes unstable when the effective temperature has cooled to a critical value that depends on the luminosity. This is theoretically reasonable but was first noticed empirically (see Humphreys and Davidson 1984, and references therein). Stars at the limit suffer rapid unsteady mass loss in sporadic outbursts; P Cyg, the Hubble-Sandage variables in M31 and M33, the S Dor variables in the LMC, and  $\eta$  Car are likely examples, among which  $\eta$  Car is one of the most luminous. There are two most plausible reasons for the observed stability limit: (1) These star's atmospheres are very near the Eddington limit set by actual opacities (not just electron scattering). Their effective opacities increase as their temperatures decrease; hence they encounter the Eddington limit while evolving at roughly constant luminosities (Lamers 1985; Humphreys and Davidson 1979; Davidson 1971). (2) De Jager (1980, 1984; see also Maeder 1983) proposed an analogous effect involving the pressure of turbulence rather than of radiation.

Thus the unique astrophysical significance of  $\eta$  Car lies in a combination of circumstances: (1) Among the known stars at the limit mentioned above,  $\eta$  Car is one of the most luminous and also one of the closest and easiest to observe. Its distance is

<sup>1</sup> Guest Investigator, IUE satellite, sponsored by NASA, the Space Research Council of the United Kingdom, and the European Space Agency.

<sup>2</sup> Visiting Astronomer, Cerro Tololo Inter-American Observatory, operated by AURA, Inc., under contract with NSF.

around 2.5 kpc (see, e.g., Walborn 1973; Feinstein, Marraco, and Muzzio 1973; Forte 1978; Thé *et al.* 1980; Thé, Bakker, and Antalova 1980). (2) We know its luminosity directly from infrared observations, without the large ultraviolet extrapolation or bolometric correction that is necessary for the O3 and most other early-type stars. (3) It has undergone a fairly recent major outburst, observed 150 years ago. (4) The outermost ejecta from this eruption, and perhaps from earlier events, may indicate the star's surface composition without too many difficulties in analysis.

Despite its importance and uniqueness,  $\eta$  Car has been studied surprisingly little at visual and ultraviolet wavelengths in recent years. In this paper we present various data, especially visual-wavelength and ultraviolet spectroscopy of the "S condensation," where earlier data were significant but crude (Davidson, Walborn, and Gull 1982; Viotti *et al.* 1981). Among other points, the S condensation provides an estimate of the helium abundance at the surface of the star in its present evolutionary state. We have also obtained data on some other outer condensations, on the "homunculus" of inner ejecta, and on the star itself.

In § II we describe our observations, mainly ground-based spectroscopy and observations with the *International Ultraviolet Explorer (IUE)* satellite. In § III we discuss the S-condensation in particular, which poses an interesting problem for astrophysicists who construct models of regions ionized by shock fronts. In § IV we briefly discuss the visible surface associated with the star itself, for our simplest view of this may conceivably be invalid. Some authors have questioned the circa 30,000 K temperature estimate; others have conjectured that the radiating surface is located in a dense stellar wind far outside the star itself, or else in an accretion disk; a binary star system might be involved. These points of uncertainty are discussed in § IV. Finally, in § V we summarize the implications of our data and we suggest observations and calculations that deserve to be undertaken in the near future.

## II. OBSERVATIONS

Figure 1 is a sketch map centered on  $\eta$  Car itself. Around the star is the  $10'' \times 16''$  "homunculus" (whose head is marked "H"), and farther out are condensations that we have labeled

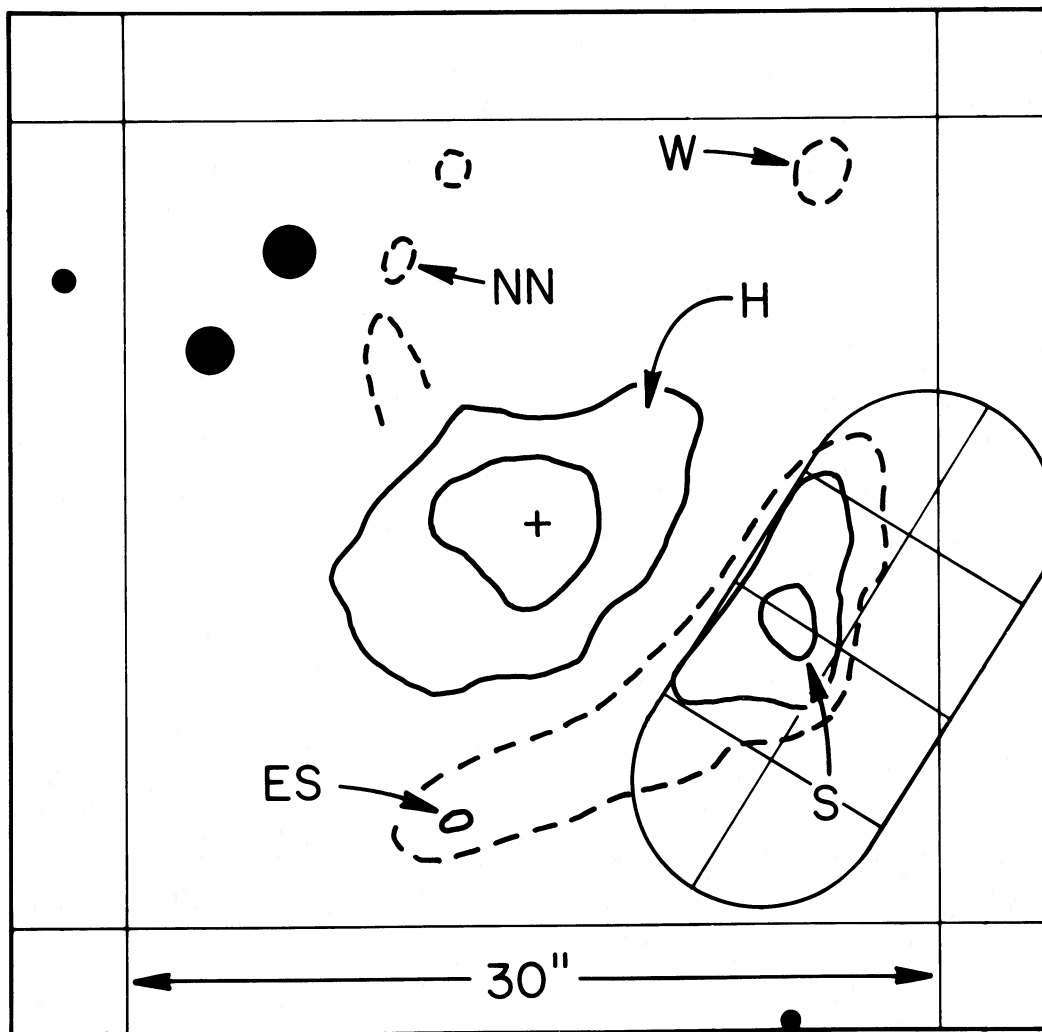


FIG. 1.—Sketch map of ejecta from  $\eta$  Car. North is at the top, east is at the left. The filled black circles are other stars. The racetrack-shaped oval represents the large aperture in *IUE* exposure SWP 18503.

with the notation used by Walborn (1976) and Walborn, Blanco, and Thackeray (1978). Observed proper motions of these condensations leave no doubt that they are ejecta from the star. Figure 2 is a contour map showing logarithms of  $H\alpha$  plus  $[N\ II]$  emission line intensities. Data for this map were obtained by one of us (K. D) on 1981 February 13, using the Cerro Tololo Inter-American Observatory 1.5 m telescope and SIT Vidicon with an interference filter. Several integrations with different exposure times were taken and were combined later, taking the nonlinear instrumental response into account. (The highest intensity levels are quantitatively doubtful.) The data were also processed to remove the background level, geometrical distortion, and a faint halo in the point spread function. The PSF in this map is nearly proportional to  $\exp[-(r/1''.12)^2]$ ; seeing was mediocre during the night of observation, and no resolution enhancement has been done except the halo removal.

Spaces between contours in the map are shaded white, gray, and black to indicate gradient directions and to make it easier to count contours. The contour interval is 0.200 in the decimal log, corresponding to a factor of 1.58 in intensity. The interference filter's transmittance curve was almost flat-topped, so

for practical purposes Figure 2 may be taken to represent simply an integrated surface brightness  $\Phi = \int I_\lambda d\lambda$  between wavelengths 6532 and 6624 Å. Calibration was done via the star CPD  $-59^\circ 2628$  (which, though not included in Fig. 2, was in the original image field), supplemented by the two stars  $13''$  northeast of  $\eta$  Car.  $UBV$  data by Feinstein, Marraco, and Muzzio (1973), who numbered these three stars as 1, 64, and 65 in the cluster Trumpler 16, were extrapolated to 6578 Å with an assumed correction factor of 0.9 for  $H\alpha$  absorption; but more importantly, R. P. Stone kindly obtained and provided absolute flux data on CPD  $-59^\circ 2628$ , which proved to be reasonably consistent with the extrapolation guess. As a reference level in Figure 2, we adopt the white/black contour just outside the S-ES "ridge," as marked with a small arrow in the figure. Our calibration gives  $\Phi = 1.75 \pm 0.12 \times 10^{-12}$  ergs  $\text{cm}^{-2} \text{s}^{-1} \text{arcsec}^{-2}$  for this level, corrected for terrestrial atmospheric extinction but not for interstellar extinction.

Figure 2 is dominated by  $H\alpha$  emission in the homunculus and by  $[N\ II]$  emission in the outlying condensations. In a similar map representing 6000 Å continuum without emission lines—i.e., light scattered by dust—the outer condensations, S in particular, are very faint; see Figure 12 of van Genderen and

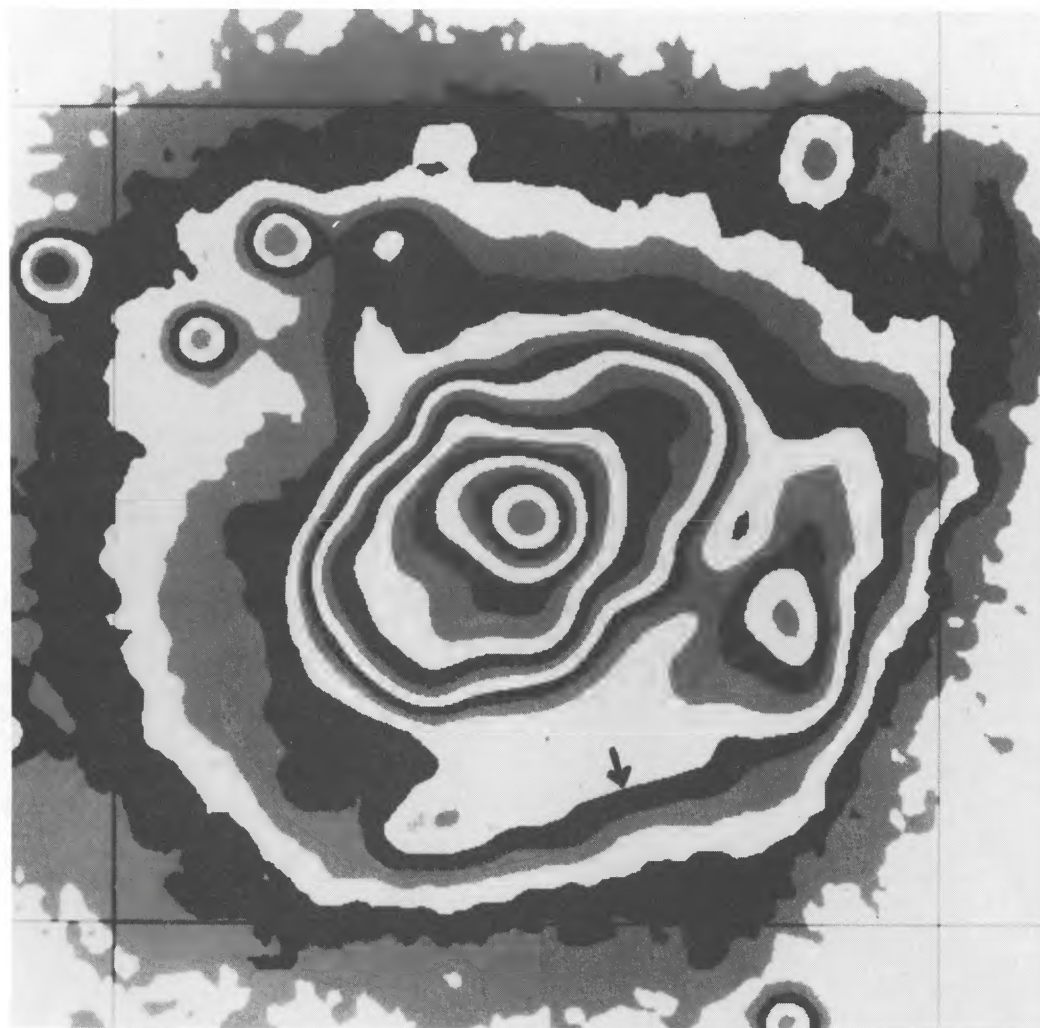


FIG. 2.—Logarithmic isophote map of  $H\alpha$  and  $[N\ II]$  emission around  $\eta$  Car. North is at the top, east is at the left, and the grid lines mark a  $30''$  square (cf. Fig. 1). A reference isophote is marked by a small arrow; the calibration is described in the text. This image may be compared with a similar but resolution-enhanced continuum picture shown as Fig. 12 of van Genderen and Thé (1985).

Thé (1985). Processing of these images for resolution enhancement suggests that the homunculus will be a very picturesque object in high spatial resolution images obtained with space telescopes.

Visual-wavelength spectroscopy of the S and ES condensations was done by one of us (R. J. D.) on 1981 July 26. The Cerro Tololo 4 m telescope and SIT Vidicon were used to cover the wavelength range from 3600 to 7600 Å with 10 Å resolution. Seven exposures were taken, with individual integration times ranging from 1 to 30 s. In each case the 2" wide spectrograph slit was positioned visually to run through the S condensation along a position angle of 120°, which also placed the ES condensation in the slit (see Figs. 1 and 2). "Seeing" was subjectively 2"-3". For the S condensation, data were extracted from a slit segment 8.3 long. Background (notably including nebular lines that occur throughout the region) was sampled in the adjoining slit segment of the same size, just outside the S condensation and near the right edge of Figure 1 or Figure 2. Background subtraction, flux calibration via standard stars, and atmospheric extinction corrections were done in a conventional way for each individual integration. Then, in order to estimate relative line intensities in the S condensation from the whole data set, appropriate weights were assigned to each line in each exposure—for example, a bright line was best represented in the short integrations, while the longest integration was best for faint lines.

In order to compare these results with the *IUE* data discussed below, we must refer to absolute fluxes, even though this is difficult and uncertain. The oblong region marked in Figure 1 indicates the *IUE* aperture size. Along the northeast side of this region is a 5" × 10" half-square which encloses the S condensation. We shall assess the H $\alpha$  plus [N II]  $\lambda\lambda 6548, 6583$  flux coming from this half-square, using three independent estimates. (1) Integration of the data shown in Figure 2 gives  $2.2 \pm 0.3 \times 10^{-10}$  ergs cm $^{-2}$  s $^{-1}$ , where we have used the flux calibration quoted earlier. (2) The H $\alpha$  + [N II] flux measured within the sampled 2" × 8.3 spectrograph slit segment was about  $1.0 \times 10^{-10}$  ergs cm $^{-2}$  s $^{-1}$ , and from this a crude estimate, involving "seeing" and the size of the condensation in the data, gave  $2.7 \times 10^{-10}$  ergs cm $^{-2}$  s $^{-1}$  for the condensation, without reference to Figure 2. (3) In March 1984, one of us (R. J. D.) obtained additional data using a wider slit. We cannot discuss these data here (they are complicated and are not yet completely reduced) except to say that in a 5.2 × 5.7 rectangle oriented northeast-southwest and centered on S, the measured H $\alpha$  + [N II] flux was  $0.94 \times 10^{-10}$  ergs cm $^{-2}$  s $^{-1}$ . From this, and relative integrations in Figure 2, we estimate  $1.3 \times 10^{-10}$  ergs cm $^{-2}$  s $^{-1}$  for the region of interest. Thus our three independent estimates span a factor of 2. Estimates (1) and (3) are best, and without further ado we assume that the apparent H $\alpha$  + [N II]  $\lambda\lambda 6548, 6583$  flux from the specified half-square enclosing the S condensation is  $1.9q \times 10^{-10}$  ergs cm $^{-2}$  s $^{-1}$ , where the factor  $q = 1.0 \pm 0.2$  will be retained below to remind us of its uncertainty.

This having been stipulated, the estimated apparent line fluxes are listed in the second column of Table 1. These refer to the half-square mentioned above and have been corrected for atmospheric extinction but not for interstellar extinction. Note that the main data for these values come, essentially, from a 4" wide strip (slit width plus seeing); errors may arise from gradients in relative line intensities across the S condensation. A number of emission lines, mostly due to Fe $^{+}$  and Fe $^{++}$ , have been omitted from Table 1.

TABLE 1  
EMISSION LINE FLUXES FROM THE S CONDENSATION<sup>a</sup>  
( $10^{-12}$  ergs cm $^{-2}$  s $^{-1}$ )

Line	Apparent Flux	Corrected for $E_{B-V} = 0.60$
N v $\lambda 1240$ .....	0.9 <i>p</i>	460 <i>p</i> :
Si iv $\lambda 1397$ .....	0.4 <i>p</i>	116 <i>p</i> :
N iv] $\lambda 1485$ .....	0.6 <i>p</i>	137 <i>p</i> :
C iv $\lambda 1549$ .....	(0.1 <i>p</i> ?)	(20 <i>p</i> ?)
He ii $\lambda 1640$ .....	0.4 <i>p</i>	66 <i>p</i> :
S iii? $\lambda 1729?$ .....	0.3 <i>p</i> :	45 <i>p</i> :
N iii] $\lambda 1750$ .....	1.8 <i>p</i>	266 <i>p</i> :
Si iii $\lambda 1888$ .....	0.7 <i>p</i>	105 <i>p</i> :
C iii] $\lambda 1908$ .....	0.14 <i>p</i> :	21 <i>p</i> :
Mg ii $\lambda 2798$ .....	(2.?)	(100 ?)
[O ii] $\lambda 3727$ .....	0.13 <i>q</i> :	3.1 <i>q</i> :
[Ne iii] $\lambda 3868$ .....	0.44 <i>q</i>	9.4 <i>q</i>
H i, He i $\lambda 3889$ .....	0.59 <i>q</i>	13 <i>q</i>
[S ii]? $\lambda 4072$ .....	1.41 <i>q</i>	26 <i>q</i>
H $\delta$ $\lambda 4102$ .....	0.64 <i>q</i>	12 <i>q</i>
H $\gamma$ $\lambda 4340$ .....	1.40 <i>q</i>	22 <i>q</i>
He i $\lambda 4472$ .....	0.24 <i>q</i>	3.5 <i>q</i>
He ii $\lambda 4686$ .....	0.09 <i>q</i> :	1.2 <i>q</i> :
H $\beta$ $\lambda 4861$ .....	4.15 <i>q</i>	49 <i>q</i>
He i $\lambda 5016$ .....	0.39 <i>q</i> :	4 <i>q</i> :
[N i] $\lambda 5199$ .....	1.92 <i>q</i>	19 <i>q</i>
[N ii] $\lambda 5755$ .....	2.9 <i>q</i>	22 <i>q</i>
He i $\lambda 5876$ .....	1.08 <i>q</i>	7.7 <i>q</i>
[N ii] $\lambda 6548$ .....	42 <i>q</i>	226 <i>q</i>
H $\alpha$ $\lambda 6563$ .....	24 <i>q</i>	128 <i>q</i>
[N ii] $\lambda 6583$ .....	124 <i>q</i>	658 <i>q</i>
He i $\lambda 6678$ .....	0.46 <i>q</i>	2.4 <i>q</i>
[S ii] $\lambda 6716$ .....	2.4 <i>q</i>	12 <i>q</i>
[S ii] $\lambda 6731$ .....	4.0 <i>q</i>	20 <i>q</i>
He i $\lambda 7065$ .....	0.63 <i>q</i>	2.8 <i>q</i>
[O ii]? } $\lambda 7324$ .....	2.2 <i>q</i>	9 <i>q</i>
[Ca ii]? }		

<sup>a</sup> These represent energy fluxes from a 5" × 10" half-square region shown in the northeast (left) side of the oblong figure in Fig. 1.

Low-resolution *IUE* data were acquired on 1982 November 7–12. We obtained short-wavelength (SWP, 1200–1950 Å) and long-wavelength (LWR, 1900–3200 Å) exposures using the large (10" × 20") and small (3" diameter) *IUE* spectrograph apertures. The size and orientation of the large aperture is shown as an oblong shape in Figure 1; the position angle of the long axis varied between 145° and 151°, and 149° may be taken as the average orientation. Our useful *IUE* exposures are listed in Table 2. Usually the large aperture center was intentionally offset from the center of the target object. For example, in SWP 18534 the W condensation was in the northern part of the aperture, while the edge of the homunculus protruded into the southern part of the aperture. Table 3 is a list of positions of the condensations that we observed; these positions are extrapolated in time from data given by Walborn, Blanco, and Thackeray (1978) and from positions in the 1981 SIT images.

The short-wavelength spectra are most interesting. Figures 3 and 4 show some of these; their implications will be discussed later. Figure 3a shows the sum of our two SWP exposures on the "core," while Figure 3b represents the northwest edge of the homunculus as found in SWP 18541. Flux values are not shown in Figure 3, because the spatial coverage is ill defined; typical intensity levels in Figures 3a and 3b differ considerably, being almost two orders of magnitude brighter in 3a. Figure 4 shows spectra of the S, ES, W, and NN condensations. These represent regions somewhat smaller than 10" × 10"; the S con-

TABLE 2  
IUE OBSERVATIONS OF  $\eta$  CARINAE, 1982 NOVEMBER 7-12

IUE Exposure Number <sup>a</sup>	Aperture <sup>b</sup>	Aperture Center <sup>c</sup>	Targets	Integration Time (minutes)
<b>SWP:</b>				
18494	Small	0, 0	Core	1
18495	Small	4"W, 3"N	H	10
18503	Large	12"W, 5"S	S	120
18505	Small	4"W, 3"N	H	35
18528	Large	5"E, 18"S	ES	120
18529	Small	5"E, 9"N	NN	120
18533A <sup>d</sup>	Large	11"W, 9"S	S	80
18533B <sup>d</sup>	Large	14"W, 2"S	S	80
18534	Large	10"W, 12"N	H, W	178
18539	Small	0, 0	Core	2
18540	Large	14"W, 3"S	S	180
18541	Large	10"W, 11"N	H, W	30
<b>LWR:</b>				
14578	Small	0, 0	Core	1
14581	Large	13"W, 5"S	S	60
14583	Small	0, 0	Core	0.3
14584	Small	4"W, 3"N	H	10
14605	Large	10"W, 3"S	S	30
14610	Large	14"W, 3"S	S	40
14611	Large	10"W, 12"N	H, W	30

<sup>a</sup> "SWP" indicates short-wavelength exposure 1200-1950 Å; "LWR" indicates long-wavelength, 1900-3200 Å.

<sup>b</sup> Small aperture, 3" diameter; large aperture, about 10" × 20" with long axis approximately along position angle 149° for our observations.

<sup>c</sup> Aperture locations are relative to the core of  $\eta$  Car in 1950 system (see Table 3).

<sup>d</sup> SWP 18533 was an intentional double exposure, placing the S condensation in two different parts of the aperture.

condensation is shown in Figures 5 and 6 and will be discussed more below. Our previous, cruder spectra of "S" (Davidson, Walborn, and Gull 1982; see also Viotti *et al.* 1981) included more scattered light from the homunculus. Note, by the way,

TABLE 3  
ADOPTED LOCATIONS AROUND  $\eta$  CARINAE<sup>a</sup>

CONDENSATION	POSITION RELATIVE TO CORE <sup>b</sup>	
	East-West <sup>c</sup>	North-South
S	9.9 W	3.8 S
ES	3.1 E	11.4 S
NN	4.8 E	10.4 N
W	10.4 W	13.3 N

<sup>a</sup> Time 1982.8; coordinate orientation 1950.

<sup>b</sup> Core position (1950.0):  $\alpha = 10^{\text{h}}43^{\text{m}}06^{\text{s}}.90$ ,  $\delta = -59^{\circ}25'15''.9$ .

<sup>c</sup> 1" = 7".63.

that each condensation has a significant ultraviolet continuum in Figure 4.

At present we are most interested in the S condensation (Figs. 5 and 6). Our relevant data were taken with S in the eastern part of the IUE spectrograph aperture. The reason for this offset, of course, was to minimize scattered light from the homunculus. If there is such contamination in the short-wavelength data, Si II  $\lambda$ 1531, which is prominent in the homunculus but not in S, will be present (compare Figs. 3, 4, and 5, and Fig. 4 of Davidson, Walborn, and Gull 1982). Since this feature is not evident in SWP 18533 and SWP 18540, they are indeed representative of the S condensation—except that some light has been lost because the center of S is so close to the aperture edge. For an absolute flux normalization we use SWP 18503, which more surely included the whole S condensation and whose location is shown by the oblong region in Figure 1. SWP 18503 is somewhat contaminated by light from the homunculus (Si II  $\lambda$ 1531 is present); but N v  $\lambda$ 1240, N IV]  $\lambda$ 1485, and He II  $\lambda$ 1640 clearly come from the condensation and not from the homunculus (what looks like homunculus N v emission in Fig. 3b is actually at 1230 Å), so their fluxes can be used. The correction factor to be applied to the uncon-

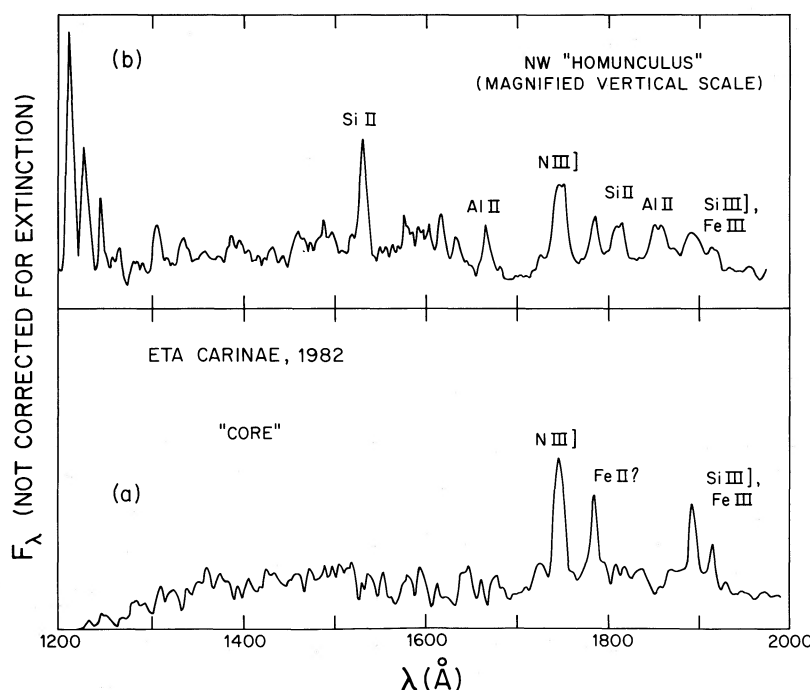


FIG. 3.—IUE spectra of  $\eta$  Car. (a) The "core"; small-aperture exposures SWP 18494 and SWP 18539 combined. (b) The northwest end of the homunculus in exposure SWP 18541. Numerical values for  $F_{\lambda}$  are omitted because these depend strongly on the spatial coverage, which is uncertain for these data.

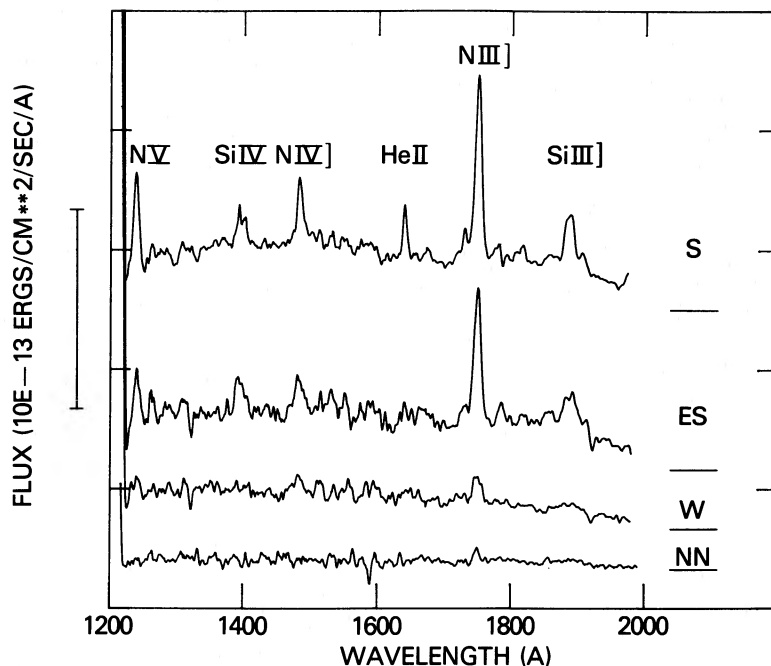


FIG. 4.—*IUE* spectra of the outer condensations labeled in Fig. 1. Zero levels are shown as horizontal lines below the condensation names.

taminated SWP 18533 and 18540 spectra was thereby found to be  $\sim 1.7$ . Extracting appropriate segments of the aperture for each *IUE* exposure, we thus find the spectrum of the  $10'' \times 10''$  square marked in Figure 1. However, we wish to refer to the northeast half of this square, as adopted above for the visual-wavelength fluxes. Based on numerical integrations in Figure 2, we assume that this half-square accounts for about 90% of each emission line flux from the entire square; with this assumption and with crude estimates of the *IUE* spatial resolution regarding its effective coverage in Figure 2, we have estimated the apparent fluxes in our standard  $5'' \times 10''$  half-square. A similar procedure can be applied to the long-wavelength *IUE* data, but the homunculus is relatively more troublesome in this wavelength range, and so the degree of

contamination may be worse. Obviously, we have made many unverifiable though plausible assumptions here, and to each flux value we attach an ultraviolet normalization uncertainty factor  $p \approx 1.0 \pm 0.2$ , analogous to the visual-wavelength factor  $q$  mentioned earlier. Some resulting ultraviolet emission line fluxes are listed in the second column of Table 1. The suspected C IV  $\lambda 1549$  feature is questionable, but the C III]  $\lambda 1908$  feature is probably real. The Mg II  $\lambda 2798$  flux is uncertain, because it may include a large scattered contribution from the homunculus. Several Fe II features are omitted for the same reason. For instance, in LWR 14610, Fe II lines between 2725 Å and 2775 Å have a total flux about one-third that of Mg II  $\lambda 2798$ .

In § IV we shall have use for some specialized photometry of  $\eta$  Car done by one of us (K. D.), using the Cerro Tololo 0.9 m

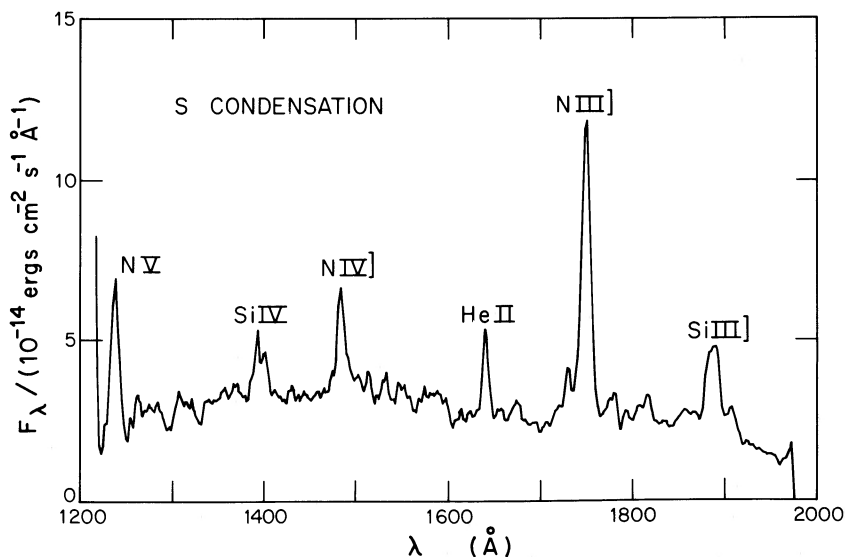


FIG. 5.—The 1200–1950 Å spectrum of the S condensation, combining *IUE* exposures SWP 18533 and SWP 18540.

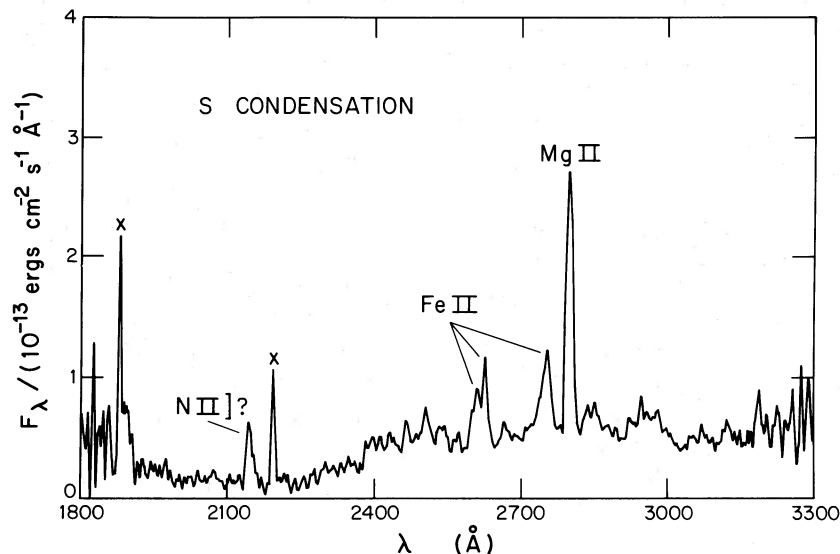


FIG. 6.—The 1900–3200 Å spectrum of the S condensation, combining *IUE* exposures LWR 14581, 14605, and 14610. Sharp features marked with crosses are instrumental defects. This spectrum may be contaminated by scattered light from the homunculus.

telescope with interference filters and a 22" photometer aperture. Absolute fluxes were calibrated by reference to HD 93250 (Thé *et al.* 1980). Observed fluxes on 1981 March 18 were  $F_{\lambda}(4700 \text{ \AA}) = 10^{-10.85} \text{ ergs cm}^{-2} \text{ s}^{-1} \text{ \AA}^{-1}$  and  $F_{\lambda}(6900 \text{ \AA}) = 10^{-10.80} \text{ ergs cm}^{-2} \text{ s}^{-1} \text{ \AA}^{-1}$ . These wavelengths were chosen to represent continuum with only slight emission-line contributions. Corrections for atmospheric extinction but not for interstellar extinction have been applied. A large number of relative measurements were made over a 5 day period, and both the fluxes just quoted were observed to be increasing at a rate of  $\sim 0.27\% \text{ day}^{-1}$ . (This was faster than the secular trend over several years; the *V*-magnitude behavior has been described by van Genderen and Thé 1985 and by Bateson, quoted by Whitelock *et al.* 1983.)

Zanella, Wolf, and Stahl (1984) have noted that the emission-line spectrum of  $\eta$  Car fluctuated during 1981, the year of our ground-based observations. However, the continuum did not change very much, and there is no reason to think that the S condensation was much affected by fluctuations in the core region.

### III. THE S CONDENSATION

Aside from uncertainties in spatial coverage, there are two practical difficulties in analyzing the spectrum of the S condensation as listed in Table 1. First, we believe that the gas is heated and ionized in a shock, which is more complicated than a simple H II region ionized by starlight; and second, we are unsure of the ultraviolet extinction corrections. Emission-line energy fluxes that have been corrected for extinction in a tentative way are listed in the third column of Table 1. Here we have used the relative extinction law found by Thé *et al.* (1980) for HD 93250, a very luminous star associated with  $\eta$  Car; this extinction is anomalous, having  $A_V/B_{B-V} = 3.9$  and a weaker than "normal" 2200 Å feature. We have assumed  $E_{B-V} = 0.60$ , a value such that the Balmer lines have theoretical "case B recombination" ratios (see below). The corrected Balmer lines are consistent enough to indicate that they are indeed due to recombination rather than to collisional excitation of H<sup>0</sup>. The corrected He I lines also have roughly "case B" ratios, except that  $\lambda 7065$  is too bright—perhaps indi-

cating an optical depth of the order of 10 for He I  $\lambda 3889$  photons. Altogether, we think that the corrected *relative* intensities of the *visual wavelength* lines are fairly reliable, at least for the region sampled by the spectrograph slit; the ultraviolet lines may be less reliable, because their extinction corrections are more uncertain.

We can estimate a few characteristic parameters for gas in S from the visual-wavelength line ratios. First, with ionic parameters from Seaton (1975) and Nussbaumer and Rusca (1979), the [N II]  $\lambda 5755/\lambda 6548, 6583$  intensity ratio gives a characteristic temperature  $T_{[N II]}$  that is between 11,700 K and 14,700 K, the most likely value being  $\sim 13,500$  K. Then, using parameters given by Mendoza (1983), Mendoza and Zeppen (1982), and Pradhan (1978), we can estimate electron densities from the [S II] lines. The  $\lambda 6731/\lambda 6716$  intensity ratio gives limits  $10^{3.2} \lesssim n_e \lesssim 10^{4.6} \text{ cm}^{-3}$  for a characteristic density in the low-ionization gas, with values around  $10^{3.6} \text{ cm}^{-3}$  preferred. The blue/red [S II]  $\lambda 4072/\lambda 6724$  line ratio indicates  $n_e \approx 10^{4.2} \text{ cm}^{-3}$  in the same gas, if  $T \approx 10,000\text{--}15,000$  K.

Continuing in this mildly naive vein, let us imagine the main part of the S condensation to be a sphere 4", or 0.05 pc, in diameter. (This size is estimated from Fig. 2 with a correction for seeing.) Slightly more than half the flux in Table 1 comes from this sphere; the H $\beta$  luminosity of the sphere is thus  $\sim 10^{34.3} \text{ ergs s}^{-1}$ . Assuming that the H $\beta$  emission is indeed due to recombination at temperatures of the order of 13,500 K, we find an emission measure of  $10^{6.8} \text{ pc cm}^{-6}$  through the sphere, an rms electron density  $n_e \approx 10^{4.1} \text{ cm}^{-3}$ , and an ionized mass of roughly  $0.03\epsilon^{1/2} M_{\odot}$ , where  $\epsilon$  is a volume-filling factor which is most likely between 0.2 and unity.

Further analysis should be done through self-consistent ionization models, probably dominated by at least one shock front. Such calculations are beyond the scope of this paper. However, we can make some very simple abundance estimates with the understanding that gradients in temperature, density, and ionization make these uncertain. Let us begin with the helium abundance, which is very important and for which we do not have to know the temperature structure very well. Considering the H $\alpha$ , H $\beta$ , H $\gamma$ , H $\delta$ , and He I  $\lambda\lambda 4472, 5876, 6678$  lines with appropriate relative weights, and using case B recombi-

nation emissivities around  $T \approx 13,500$  K, we derive  $n(\text{He}^+)/n(\text{H}^+) = 0.14 \pm 0.01$  from the third column of Table 1. The weakness of the He II  $\lambda 4686$  recombination line shows that  $n(\text{He}^{+2})/n(\text{H}^+)$  is negligible in the observed gas (we mention He II  $\lambda 1640$  later). Corrections for  $\text{He}^0$  and  $\text{H}^0$ , mainly  $\text{He}^0$  coexisting with  $\text{H}^+$ , are difficult to make without elaborate models. Based on the nitrogen ionization (see below), we suspect that  $n(\text{He})/n(\text{H}) \approx 1.2n(\text{He}^+)/n(\text{H}^+) \approx 0.17$ . This estimate, essentially the same as a preliminary value that we quoted in an earlier paper (Davidson *et al.* 1984), corresponds to a helium mass fraction  $Y \approx 0.40$ , interestingly larger than in the Sun. Allen, Jones, and Hyland (1985) have found a similar result from infrared lines in the spectrum of the homunculus, where high densities make the visual wavelength helium lines difficult to analyze. The helium abundance around  $\eta$  Car, indirectly representing the outer layers of the star itself, is significant with regard to the star's evolutionary state. For instance, fitting the observed luminosity and our estimated surface He/H ratio in  $\eta$  Car to evolutionary models like those of Maeder (1983), we would conclude that the star had an initial mass near  $170 M_\odot$  and is now  $\sim 10^{6.4}$  yr old with a present mass near  $120 M_\odot$ . An important specific application of proper ionization models of the S condensation would be to derive the helium abundance more accurately from the observed  $\text{He}^+/\text{H}^+$  ratio.

Since the gas in the S condensation has been through the CNO cycle, most of the CNO is nitrogen (Davidson, Walborn, and Gull 1982). Therefore we expect, roughly,  $n(\text{N})/n(\text{H}) \approx 10^{-3}$ . The Balmer and [N II] fluxes in Table 1 give  $n(\text{N}^+)/n(\text{H}^+) \approx 1.5 \times 10^{-4}$ , including a small correction for collisional de-excitation. This suggests that most of the nitrogen is ionized beyond  $\text{N}^+$ . If we merely pretend that  $\text{N}^{+2}$ ,  $\text{N}^{+3}$ ,  $\text{N}^{+4}$ , and  $\text{H}^+$  coexist at temperature  $T$  and use the line ratios in the third column of Table 1 with collision strengths given by Mendoza (1983), Nussbaumer and Storey (1982), and Osterbrock and Wallace (1977), we find

$$n(\text{N}^{+2})/n(\text{H}^+) \approx (1.0 \times 10^{-6}) \exp [(90,000 \text{ K})/T],$$

$$n(\text{N}^{+3})/n(\text{H}^+) \approx (2.3 \times 10^{-7}) \exp [(102,000 \text{ K})/T],$$

$$n(\text{N}^{+4})/n(\text{H}^+) \approx (1.4 \times 10^{-7}) \exp [(123,000 \text{ K})/T].$$

These formulae are useful for thinking about temperatures, even though gradients in temperature, density, and ionization can partially invalidate them. We expect that the characteristic temperatures for different types of emission may be different,  $T_{\text{H}\beta} \lesssim T_{\text{N III}} \lesssim T_{\text{N III}} \lesssim T_{\text{N IV}} \lesssim T_{\text{N V}}$ . In fact, if we merely assume  $T = T_{\text{N III}} \approx 13,500$  K in all these formulae, a rather high total nitrogen abundance results,  $n(\text{N})/n(\text{H}) > 10^{-2.7}$ . Higher temperatures of the order of 16,000 K for  $\text{N}^{+2}$ ,  $\text{N}^{+3}$ , and  $\text{N}^{+4}$  give plausible values,  $n(\text{N})/n(\text{H}) \approx 10^{-3}$ . The  $\text{N}^{+3}$  and  $\text{N}^{+4}$  temperatures may be higher, but the characteristic temperature for  $\text{N}^{+2}$  probably does not exceed 18,000 K; otherwise the total nitrogen abundance is found to be surprisingly low. This last statement is valid even if the N III], N IV], and N V emission arise in zones that are spatially distinct from the main provenance of the hydrogen Balmer line emission.

For other elements, let us use collision strengths from many references cited by Mendoza (1983). Unless otherwise noted, we assume that  $T \approx 13,500$  K for  $\text{N}^+$  and similar ions according to ionization potentials, and  $T \approx 16,000$  K for  $\text{N}^{+2}$  and similar ions. Then the (C III]  $\lambda 1908$ )/(N III]  $\lambda 1750$ ) line ratio indicates  $n(\text{C}^{+2})/n(\text{N}^{+2}) \approx 0.02$ . The C IV  $\lambda 1549$  intensity given

in Table 1 may be illusory (a  $1 \sigma$  result), but its ratio with N IV]  $\lambda 1485$  is consistent with  $n(\text{C}^{+3})/n(\text{N}^{+3}) \approx 0.02$ . Both these carbon/nitrogen estimates are only mildly temperature-dependent, so we conclude that in the gaseous state, most likely  $n(\text{C})/n(\text{N}) \approx 0.02$  in the S condensation.

Oxygen is a more complicated case. The  $\lambda 7324$  feature in Table 1 is probably not mainly [O II]; it is too narrow to represent the [O II] quadruplet, and the  $\lambda 7324/\lambda 3727$  ratio would indicate too high a density. The [O II]  $\lambda 3727$  doublet is probably affected by collisional de-excitation. Its intensity relative to the [N II] lines indicates that the abundance ratio  $n(\text{O}^+)/n(\text{N}^+)$  is, very roughly,  $\sim 0.006 [1 + n_e/(10^4 \text{ cm}^{-3})] \approx 0.015(?)$ , where  $n_e$  is the electron density in the [N II], [O II]-emitting gas. Doubly ionized oxygen is absent from our data when nebular background is removed; the ([O III]  $\lambda 5007$ )/([N III]  $\lambda 1750$ ) intensity ratio in S appears to be less than 0.02 after correction for extinction. This would imply  $n(\text{O}^{+2})/n(\text{N}^{+2}) \lesssim 0.007$ ; however, [Ne III]  $\lambda 3868$  is surprisingly weak in our data, suggesting the possibility that the slit used for our ground-based spectroscopy might not have sampled the doubly ionized species well enough. There is no doubt that  $\text{O}^{+2}$  is scarce; the absence of a perceptible  $\lambda 5007$  line and presence of the  $\lambda 3868$  line show that there is much less oxygen than neon. It seems fair to conclude that  $n(\text{O}^{+2})/n(\text{N}^{+2}) < 0.05$ . Independent of ground-based data, the absence of [O III]  $\lambda 1664$  in the IUE data gives a very cautious limit  $n(\text{O}^{+2})/n(\text{N}^{+2}) < 0.25$ .

Emission lines of silicon give indirect hints about oxygen and nitrogen in the S condensation. If material is not heavily processed in  $\eta$  Car beyond the CNO cycle, then silicon should have a more or less "normal" abundance. Our Si III]  $\lambda 1888$  and Si IV  $\lambda 1397$  fluxes indicate, roughly,  $n(\text{Si}^{+2}, \text{Si}^{+3})/n(\text{H}^+) \approx 10^{-4.5 \pm 0.3}$ , where much of the uncertainty arises from the strong temperature dependence of the ultraviolet lines. A "normal" Population I silicon abundance would be of the order of  $n(\text{Si})/n(\text{H}) \approx 10^{-4.5}$ . Evidently, then, a large fraction of the silicon is gaseous, not in dust grains, even though silicate grains have formed around  $\eta$  Car (see, e.g., Thomas, Robinson, and Hyland 1976). Maybe this indicates that the overall oxygen/silicon abundance ratio is considerably less than 2 by number. Then the formation of silicates would have been limited by the amount of oxygen, "excess" silicon would remain gaseous, and there would be little gaseous oxygen. This would imply that  $n(\text{O})/n(\text{H}) \lesssim 10^{-4.2}$ , referring to the total, not just gaseous, oxygen. (Admittedly, this argument leaves it unclear why we see detectable [O II] emission.)

Let us continue the silicon train of thought just a bit further, to encompass nitrogen. Roughly speaking,  $\text{Si}^{+2}$  should coexist with  $\text{N}^+$ , and  $\text{Si}^{+3}$  with  $\text{N}^{+2}$ . The Si III]/[N II] and Si IV/N III] line ratios in Table 1 indicate that  $n(\text{Si}^{+2})/n(\text{N}^+)$  is of the order of 0.05–0.1, while  $n(\text{Si}^{+3})/n(\text{N}^{+2}) \approx 0.05$ . The latter result is not very temperature-dependent and may represent a large fraction (perhaps half) of the gaseous silicon and nitrogen. If  $f$  is the fraction of silicon that is gaseous, then we estimate an overall abundance ratio  $n(\text{Si})/n(\text{N}) \approx 0.05/f$ . If the silicon abundance is "normal," then this gives an indirect estimate of the nitrogen abundance, which accounts for most of the CNO:  $n(\text{N})/n(\text{H}) \approx 10^{-3.2f}$ . If  $f$  is close to unity, then this crude estimate of the CNO abundance is roughly normal for Population I, or perhaps slightly low. If  $f$  is much less than unity, then the CNO abundance is unexpectedly low.

Although the situation as discussed so far seems reasonably consistent, there are some disquieting anomalies in Table 1.

Perhaps the worst involves the He II  $\lambda\lambda 1640, 4686$  lines. If these are both due to recombination, the  $\lambda 1640/\lambda 4686$  intensity ratio should be close to 7 (Seaton 1978); but in the third column of Table 1 this ratio is much higher,  $\sim 55$ . Most obvious possible explanations for this discrepancy seem unsatisfactory to us. (1) Conceivably the  $\lambda 1640$  emission results mainly from collisional excitation of ground-level He<sup>+</sup> by thermal electrons. But this would require high temperatures,  $T \gtrsim 45,000$  K, in some of the He<sup>+</sup> gas. At such temperatures,  $\lambda 4686$  would also be excited in the same way, and it would be difficult to get a  $\lambda 1640/\lambda 4686$  intensity ratio much larger than 30. Besides, N III]  $\lambda 1750$  and N IV]  $\lambda 1485$  would be produced so efficiently that our data would imply a surprisingly small nitrogen abundance. (2) Partial photoionization of He<sup>+</sup> by soft X-rays and subsequent recombination, along with trapping of He II  $\lambda 304$  resonance photons, might elevate the population of He<sup>+</sup> ions in the  $n = 2$  level, from which excitation to  $n = 3$ , producing  $\lambda 1640$ , can occur at relatively modest temperatures. However, this explanation requires an implausibly small escape-or-destruction probability for  $\lambda 304$  photons. (3) Maybe  $\lambda 4686$  emission (He<sup>+</sup>, level  $n = 4$  to  $n = 3$ ) is somehow inhibited. One might imagine making use of the near-coincidence between H I Ly $\alpha$  and the H $\beta$ -like He II  $\lambda 1215$  transition to de-excite the  $n = 4$  level of He<sup>+</sup>. Quantitatively, though, this idea does not work. Effects like this have been discussed with regard to quasars (many references are cited by Davidson and Netzer 1979 and MacAlpine *et al.* 1985), and such effects are usually not strong for the He II lines even at the high densities associated with quasars. (4) Maybe we have overestimated the ultraviolet extinction correction in Table 1, and the intrinsic  $\lambda 1640/\lambda 4686$  line ratio is considerably less than 55. Then the extinction at  $1640 \text{ \AA}$  would not be much stronger than at  $4000 \text{ \AA}$ . If so, however, the ultraviolet nitrogen lines are also weaker than we have supposed, leading to a surprisingly small nitrogen abundance. A downward reassessment of the average ionization state would also follow, making the visual wavelength He I recombination lines difficult to understand. So this is not an appealing explanation either. (5) Conceivably, the high-ionization zones (He<sup>+2</sup>, N<sup>+3</sup>, N<sup>+4</sup>, etc.) were missed by the visual wavelength spectrograph slit—perhaps the high-ionization gas is 2" or 3" west of the visual wavelength center of the S condensation. This would not greatly affect our crude analysis discussed above, where we did not much use any high-ionization visual wavelength lines except for passing references to He II  $\lambda 4686$  and (lower in ionization) [O III] and [Ne III]. The He II  $\lambda 1640$  flux in Table 1 is consistent with the values for N IV]  $\lambda 1485$  and N V  $\lambda 1240$  if the high-ionization temperature is in the neighborhood of 20,000 K and if  $\lambda 1640$  is largely due to recombination. Our helium/hydrogen abundance ratio estimate, outlined earlier, is not affected, because it referred to the gas observed through the visual wavelength spectrograph slit. Pending further visual wavelength spectrophotometry, we remain somewhat puzzled by the observed He II  $\lambda 1640/\lambda 4686$  ratio. Another possible cause of this discrepancy will be mentioned later.

Our data on the S and ES condensations and the homunculus show an emission feature near  $1730 \text{ \AA}$ . In Table 1 we have labeled this as S III]  $\lambda 1729$  (Moos *et al.* 1983; Durrance, Feldman, and Weaver 1983). However, using the collision strength given by Ho and Henry (1984), we find that this requires an abundance ratio  $n(S^{+2})/n(N^{+2}) \approx 0.2$ , which seems too high by a factor of order 10. One of the strongest unidentified features noted by Penston *et al.* (1983) in high-resolution IUE data on RR Tel is at  $1732 \text{ \AA}$ .

A fairly strong continuum is present in our ultraviolet data on the S condensation and in other outer condensations as well (Fig. 4). The equivalent widths of N IV]  $\lambda 1485$  and N III]  $\lambda 1750$  in S are only about  $13 \text{ \AA}$  and  $60 \text{ \AA}$  respectively; there is far more energy flux in the apparent continuum than in the observed emission lines. Likely explanations parallel the discussion of ultraviolet continuum emission in a Herbig-Haro object by Brugel, Shull, and Seab (1982), who discussed two-photon emission by hydrogen, and by Mundt and Witt (1983), who favored reflection by dust grains. The imperfect quality of our IUE data and uncertainties in the extinction correction prevent us from quoting an accurate wavelength dependence, but it seems at least possible that this is consistent with two-photon emission in the S condensation. The value of  $\lambda F_{\lambda}$  at  $1500 \text{ \AA}$ , relative to the H $\beta$  flux, is (very roughly) 40% larger than the corresponding ratio cited by Brugel *et al.*; this may be taken to be consistent with the two-photon hypothesis, provided that the relevant electron densities are not much higher than  $10^4 \text{ cm}^{-3}$  (two-photon emission is partially suppressed at higher densities).

At the same time, reflection by dust is also quantitatively possible. The likely column density through the S condensation is of the order of  $10^{21}$  atoms and ions  $\text{cm}^{-2}$ , thick enough for dust to make it fairly opaque in the ultraviolet. The reddening indicated by the Balmer lines seems to confirm this. Feinstein, Marraco, and Muzzio (1973) found reddening values due to interstellar dust for many stars in the Trumpler 14 and 16 cluster, and from their data it appears that  $\eta$  Car is in a local minimum where  $E_{B-V} \approx 0.40$ . (Does this local minimum signify that  $\eta$  Car has cleared a space around itself? Cf. Walborn and Hesser 1975; Allen 1979.) This value of  $E_{B-V}$  does not include circumstellar reddening directly associated with ejecta from  $\eta$  Car. Since we find  $E_{B-V} \approx 0.60$  from the Balmer lines in the S condensation, the value associated with dust in the condensation itself may be as large as  $E_{B-V} \approx 0.20$ . If some of the reddening is internal, then the wavelength dependence used for corrections in Table 1 is questionable. This suggests another possible explanation for the surprisingly large  $\lambda 1640/\lambda 4686$  ratio in the third column of Table 1. Perhaps the high-ionization He II, N IV], and N V lines, coming from a less deep region in the S condensation, experience less reddening than most other lines; if so, then in Table 1 we have overcorrected these high-ionization lines. A lesser amount of internal extinction may be necessary for N V  $\lambda 1240$ , a resonance line, in order to allow  $\lambda 1240$  photons to escape without being absorbed by dust after many scattering events. Anyway, the S condensation can scatter and reflect a moderate fraction of whatever ultraviolet flux is incident upon it. Note, however, that some of the spectral features in the core and homunculus (Fig. 3) are not prominent in the spectrum of S; this fact argues against the scattering hypothesis as an explanation of the continuum of S.

#### IV. SOME REMARKS ABOUT ETA CARINAE ITSELF, AND ABOUT THE HOMUNCULUS

Most authors agree that the basic luminosity of  $\eta$  Car emerges from some opaque surface; but they do not agree about the nature of the surface or its temperature. This surface may be a true stellar photosphere, or else a location in the stellar wind, or even the surface of an accretion disk (for this last idea, see Bath 1979). Proposed values for the apparent temperature fall into four physically different categories: (a)  $T \approx 7500 \text{ K}$  (Andriesse, Packet, and de Loore 1981); (b)  $T \approx 15,000 \text{ K}$  (Pottasch, Wesseliuss, and van Duinen 1976); (c)

$T \approx 30,000$  K (Davidson 1971; see also Pagel 1969b); (d)  $T \gtrsim 40,000$  K (Allen, Jones, and Hyland 1985). The continuum should offer some clues to this question. Unfortunately, there are no proper theoretical models for comparison, as far as we know—the surface gravities assumed in various photosphere calculations that are sometimes cited have been too large to represent  $\eta$  Car. Thus, for simplicity and definiteness, we shall refer to idealized blackbody continua. This may seem naive, but we find that the observed continuum actually resembles a blackbody.

The integrated energy flux that would be observed at Earth in the absence of extinction can be estimated from infrared data with modest corrections. This flux is  $\sim 10^{-4.58}$  ergs  $\text{cm}^{-2}$   $\text{s}^{-1}$  according to van Genderen and Thé (1985), or  $10^{-4.70}$  ergs  $\text{cm}^{-2}$   $\text{s}^{-1}$  according to Harvey, Hoffman, and Campbell (1978). Here we adopt  $10^{-4.68}$  ergs  $\text{cm}^{-2}$   $\text{s}^{-1}$ , which matches the value assumed by Davidson (1971). At a distance of 2.5 kpc this corresponds to a luminosity of  $10^{6.61} L_{\odot}$ , or bolometric magnitude  $M_{\text{bol}} \approx -11.78$ .

Now consider the observed ultraviolet and visual continuum. In our small-aperture *IUE* data on the “core” of  $\eta$  Car,  $F_{\lambda} \approx 10^{-11.4}$  ergs  $\text{cm}^{-1}$   $\text{s}^{-1}$   $\text{\AA}^{-1}$  at  $\lambda \approx 1500$   $\text{\AA}$ . This refers to a small sampled region and very crudely suggests a value  $F_{\lambda} \approx 10^{-10.9}$  ergs  $\text{cm}^{-2}$   $\text{s}^{-1}$   $\text{\AA}^{-1}$  for the whole object. The large-aperture *IUE* data shown by Viotti *et al.* (1981), obtained 2 yr earlier than ours, appear to have  $F_{\lambda} \approx 10^{-11.15}$  ergs  $\text{cm}^{-2}$   $\text{s}^{-1}$   $\text{\AA}^{-1}$  at the same wavelength. We adopt  $F_{\lambda}$  (1500  $\text{\AA}$ ) =  $10^{-11.05}$  ergs  $\text{cm}^{-2}$   $\text{s}^{-1}$   $\text{\AA}^{-1}$ , intended to refer to the same time in 1981 as the visual wavelength data invoked below.<sup>3</sup> Absorption features make the flux lower around 1600  $\text{\AA}$  (see Fig. 3a). The 2400–2900  $\text{\AA}$  continuum is hidden beneath an Fe II emission line forest, but the *IUE* data suggest that  $F_{\lambda}$ (3000  $\text{\AA}$ ) is about twice as large as  $F_{\lambda}$ (1500  $\text{\AA}$ ). As mentioned at the end of § II, in 1981 March we found  $F_{\lambda}$ (4700  $\text{\AA}$ )  $\approx 10^{-10.85}$  ergs  $\text{cm}^{-2}$   $\text{s}^{-1}$   $\text{\AA}^{-1}$  and  $F_{\lambda}$ (6900  $\text{\AA}$ )  $\approx 10^{-10.80}$  ergs  $\text{cm}^{-2}$   $\text{s}^{-1}$   $\text{\AA}^{-1}$ . None of the fluxes just quoted has been corrected for interstellar and circumstellar extinction.

These observed values are remarkably consistent with a 30,000 K blackbody continuum having the adopted integrated energy flux and a reasonable extinction law. The required extinction values are  $A_{\lambda} \approx 2.95, 5.0,$  and  $7.6$  mag at  $\lambda = 5500, 3000,$  and  $1500$   $\text{\AA}$  respectively. The ratio  $A_{\lambda 1500}/A_V$  then matches an extinction law intermediate between a “normal” version and the Thé *et al.* (1980) “anomalous” version adopted in Table 1. (Blackbody continua with  $T \approx 33,000$  K and  $27,000$  K respectively, and with the assumed integrated flux, would exactly match the  $A_{\lambda 1500}/A_V$  ratios for these two extinction laws.) Moreover, the 3000  $\text{\AA}$  point is also satisfactory. These pleasant coincidences do not *prove* much—the data are imprecise, we do not really know how close the continuum should be to a blackbody curve, and the circumstellar extinction law is poorly known—but they are highly suggestive. For temperatures much lower than 25,000 K or much higher than 35,000 K, the required extinction ratio  $A_{\lambda 1500}/A_V$  would be implausibly small or large respectively.

What we have just said is essentially like an argument made by Davidson (1971), with three notable differences: (1) The indicated effective reddening  $E_{B-V}$  is around 0.9 mag, some-

what less than the reddening derived by Pagel (1969a), Lambert (1969), Viotti (1969), Ade and Pagel (1969), and Davidson (1971) from visual and near-infrared wavelength emission-line ratios observed during the 1960s. Very likely there was a real decrease in  $E_{B-V}$  during the 15 yr preceding 1982. This should be checked by reobserving the [Fe II] and hydrogen emission lines coming from the core and homunculus. Comparing with stars around  $\eta$  Car (Feinstein, Marraco, and Muzzio 1973), we estimate that slightly more than half the suspected reddening is circumstellar rather than interstellar. Since any appreciable change must have been circumstellar, a fairly large relative decrease in this component is suspected. (2) A second difference from Davidson (1971) is that we have used ultraviolet data. Lacking such data, the 1971 argument made use of the visual wavelength continuum slope observed a few years earlier by Rodgers and Searle (1967). Similar observations should now be done with modern equipment. The apparent visual continuum is certainly brighter than it was during the 1960s. (3) We have not yet mentioned the Zanstra-style argument which, 15 yr ago, independently suggested  $T \approx 30,000$  K for  $\eta$  Car. Allen, Jones, and Hyland (1985), using their data and those of Giles (1977), have lately estimated that this object produces at least  $10^{49.8}$  hydrogen-ionizing photons  $\text{s}^{-1}$  if its distance is 2.5 kpc (cf. Aitken *et al.* 1977, Davidson 1971). Our idealized 30,000 K blackbody would produce roughly 70% more ionizing photons than this; with a plausible Lyman continuum absorption jump (remember that this jump is not very deep, because the surface gravity is low),  $T \approx 30,000$  K seems consistent with the Zanstra argument. If this argument is indeed valid—if the relevant hydrogen is mostly photoionized by stellar radiation—then the star must be hotter than 25,000 K. As in 1971, arguments based on the photoionization heating budget may favor a temperature somewhat hotter than 30,000 K; but we shall not discuss this rather conjectural point here.

If a simple model with  $T \approx 30,000$  K is so satisfyingly consistent, we must ask what is wrong with arguments that have been made for other temperature ranges. Any effective temperature below 15,000 K is very unlikely, because a large excess of ultraviolet radiation or a shortage of visual radiation, as well as the hydrogen and helium emission-line fluxes, would have to be explained in such a model. Pottasch, Wesselius, and van Duinen (1976) proposed  $T \approx 15,000$  K for  $\eta$  Car on the basis of ultraviolet photometry acquired with the *ANS* instrument. However, the continuum, emission lines, and a nearby hot star could not be disentangled very well in their data, and their extinction correction relied heavily on an assumed “normal” 2200  $\text{\AA}$  interstellar extinction feature. This last assumption is highly questionable; see Thé *et al.* (1980). (Many astronomers during the 1970s tended to ascribe an illusory quantitative universality to the 2200  $\text{\AA}$  feature.) The apparent size of  $\eta$  Car can sometimes expand, and its effective temperature can decrease, during temporary eruptive events; but given the observed visual and ultraviolet continuum fluxes, the likely value of  $E_{B-V}$  indicated by hydrogen and [Fe II] emission line ratios, the integrated luminosity measured in the infrared, and the Zanstra argument, we are reasonably confident that the object has been hotter than 20,000 K during the 1965–1985 period.

Lacking suitable photosphere and wind models, we cannot be so confident in arguing against the high temperature proposed by Allen, Jones, and Hyland (1985). They believed that the radiating surface associated with  $\eta$  Car must be as hot as

<sup>3</sup> See also Fig. 6 of Zanella, Wolf, and Stahl (1984). One of their tracings is derived from our small-aperture *IUE* data. These authors note that the emission-line spectrum temporarily changed in 1981, but the continuum level did not change enough to affect our discussion here.

an early O-type star, in order to ionize enough helium to explain the observed He I recombination lines in the homunculus. What is required for this, essentially, is that the ratio (helium-ionizing photons)/(hydrogen-ionizing photons) must equal or exceed the ionic abundance ratio  $n(\text{He}^+)/n(\text{H}^+)$  in the homunculus, of the order of 0.13–0.18 according to Allen *et al.*<sup>4</sup> For a blackbody continuum this implies  $T > 38,000$  K; existing stellar atmosphere models would require even higher temperatures but may be inapplicable because their surface gravities are excessive. This argument has some possible defects that must be checked through detailed calculations. For example, because electron densities are high in the core of the homunculus, the physics of the observed helium emission is complicated—as Allen *et al.* note. Moreover, dust mixed with the ionized hydrogen and helium can destroy a larger fraction of the hydrogen-ionizing photons than of the helium-ionizing photons, leading one to overestimate the intrinsic stellar helium-ionizing/hydrogen-ionizing ratio. Indeed, if the effective temperature exceeds 35,000 K, then most of the ionizing photons must be destroyed by dust in order to avoid inciting much more than the observed hydrogen recombination emission. If  $T \gtrsim 40,000$  K, then a surprisingly large extinction ratio,  $A_{\lambda 1500}/A_V > 3.3$ , would be required, or in other words, the apparent ultraviolet/visual continuum flux ratio is smaller than is expected for such a hot continuum. (Given the total luminosity and the partially known value of  $E_{B-V}$ , this argument does not depend entirely on our blackbody assumption.)

Thus we favor a temperature below 40,000 K for the “visible” surface. The star itself may conceivably be hotter and surrounded by a dense opaque wind (Appenzeller 1970); but an actual stellar effective temperature around 30,000 K (possibly 35,000 K) is intuitively appealing, because this would help to explain why  $\eta$  Car is conspicuously less stable than the hotter O3 stars of comparable luminosity.

Absorption features in the IUE data (Fig. 3a) are, unfortunately, not very helpful at our simple level of discussion. We think that Si IV  $\lambda 1399$  and perhaps C IV  $\lambda 1549$  absorption are present, slightly shifted in wavelength as is appropriate for P Cygni features; these are consistent with the discussion above. Some lower ionization features (Al III  $\lambda 1860$ , perhaps Si II  $\lambda 1530$ ) also seem to be present, but these may arise in the outer, cooler parts of the stellar wind—detailed models are needed. We suspect that a P Cygni N V  $\lambda 1240$  line is also present. The complicated spectrum between 1500 and 1750 Å may prove useful when sophisticated calculations are done.

The apparent effective temperature implies a limit to the stellar wind. The continuous mass loss rate, as seen now, cannot exceed  $10^{-2.4} M_{\odot} \text{ yr}^{-1}$  if the apparent temperature is around 30,000 K or higher and the outflow speed is 700 km s<sup>-1</sup>; otherwise the opacity in the dense wind would be so great that the emergent radiation would originate too far out, i.e., too cool. Some authors have proposed far greater mass loss rates, mainly on the basis of the amount of dust believed to exist in the homunculus (Hyland *et al.* 1979; Andriessse, Donn, and Viotti 1978); but these may represent average rates over a period of many years (possibly two centuries), and a significant characteristic of mass loss from  $\eta$  Car is its notorious unsteadiness (Humphreys and Davidson 1979, 1984, and many references therein). Van Genderen and Thé (1985) have recently

proposed a mass loss rate well below  $10^{-3} M_{\odot} \text{ yr}^{-1}$  for  $\eta$  Car as seen today. For such a low mass loss rate, the observed continuum comes from the star’s surface and not from the wind.

Infrared data on the distribution of dust are obviously relevant to several points mentioned above. Since conclusions depend on specific dust grain parameters, for definiteness we simply use values given by Draine and Lee (1984) for silicate grains with radii of the order of 0.1  $\mu\text{m}$  (cf. Thomas, Robinson, and Hyland 1976). The observed infrared luminosity requires a dust mass of the order of  $10^{-2.1} M_{\odot}$  in the homunculus. Considering that oxygen and carbon are scarce there, one might fear that a very large amount of gas is required in order to produce so much dust. However, the following discussion shows that the recent grain formation rate (i.e., as we see the object today) has not been excessive.

Most of the luminosity emerges from the homunculus at wavelengths around 30  $\mu\text{m}$ , characteristic of grain temperatures around 250 K at distances of 0.03–0.07 pc from the star (Hyland *et al.* 1979; Harvey, Hoffman, and Campbell 1978; Aitken *et al.* 1977). This is presumably the dust that was seen to form around 1860 (when  $\eta$  Car became fainter at visible wavelengths), moving outward at several hundred km s<sup>-1</sup>. Since this dust must be heated mainly by the stellar ultraviolet luminosity, evidently *the inner, hotter, more recently formed dust is not optically thick in the UV*. From the observed 2–8  $\mu\text{m}$  continuum (Gehrz *et al.* 1973; Aitken *et al.* 1977; Whitelock *et al.* 1983), we estimate that less than 25% of the stellar luminosity is absorbed and reradiated by grains hotter than 500 K, and less than 10% by grains hotter than 700 K. Suppose that grains condense at temperature  $T_c$ , within an isotropic stellar wind. Then the ultraviolet transparency of the recently formed, innermost, hottest grains implies a rough limit to the rate of dust formation in terms of mass:

$$\frac{dM_d}{dt} \lesssim (10^{-5.3} M_{\odot} \text{ yr}^{-1}) \left( \frac{v}{700 \text{ km s}^{-1}} \right) \left( \frac{10^3 \text{ K}}{T_c} \right)^2 \left( \frac{a}{1 \mu\text{m}} \right)^{0.5},$$

where  $v$  is the wind speed and  $a$  is a typical grain radius (silicates with  $0.01 \lesssim a \lesssim 1 \mu\text{m}$  are assumed). Even if only 0.1% of the outflowing mass condenses into grains, this limit is consistent with the limit to the stellar mass loss rate, mentioned above.

This picture—wherein the *inner* homunculus is almost transparent at nonionizing wavelengths—seems compatible with the obvious differences between Figure 3a (the ultraviolet spectrum of the “core”) and Figure 3b (the ultraviolet spectrum of the outer homunculus). Heating and excitation in the homunculus, producing a low-ionization emission spectrum (Si II  $\lambda 1531$ , etc.), are not understood and merit theoretical study.

Velocities in the homunculus also need to be studied, because the situation is confusing. High outflow speeds of the order of 700 km s<sup>-1</sup> are indicated by Mg II and Balmer-line absorption features (see Melnick, Ruiz, and Maza 1982; Cassatella, Giangrande, and Viotti 1979, and earlier references therein). Since Balmer absorption lines cannot easily arise in moderate-density nebular conditions, we suppose that these speeds occur in the dense stellar wind and not just in outer condensations. However, the H $\alpha$  line profile (Fig. 1 of Melnick, Ruiz and Maza 1982) shows that much of the H $\alpha$ -emitting gas probably has lower outflow speeds, typically 200 or 300 km s<sup>-1</sup>. There is even a narrow central peak representing gas velocities of 100 km s<sup>-1</sup> or less, relative to the central object. The

<sup>4</sup> This requirement follows from the near-equality of hydrogen and helium recombination coefficients; here we omit details regarding photoionization structure.

size of the homunculus (Fig. 2) indicates outward speeds ranging between 300 and 700 km s<sup>-1</sup> if most of the material was ejected in the outburst seen around 1840. All together, with such a large dispersion in velocities, we may expect shocks to occur in the homunculus. But if so, then why do the emission lines in the homunculus represent such a low average ionization state, and why is the observed X-ray emission (Chlebowski *et al.* 1984) so weak?

Our confusion, or at least uncertainty, is enhanced by infrared and visual wavelength maps of the homunculus (Hyland *et al.* 1979; Mitchell *et al.* 1983; Fig. 12 of van Genderen and Thé 1985; Fig. 2 above). The “core” is comma-shaped in the visual wavelength maps and double in the infrared, while the homunculus, though lumpy, appears to be basically ellipsoidal. Obviously any assumption of spherical symmetry is at best imperfect, at worst totally erroneous. As Hyland *et al.* (1979) and Mitchell *et al.* (1983) have discussed, the homunculus may be a “bipolar” structure whose core is a toroidal accumulation of gas and dust around the main central star. If this is so, then perhaps the low-velocity H $\alpha$  emission observed by Melnick, Ruiz, and Maza (1982) arises in the toroid. Whether the hypothetical toroid covers the line of sight to the star, we cannot say; the existence and details of this structure must be investigated through high spatial resolution observations. (We should acknowledge that our upper limits to the mass loss rate can be invalidated if the mass loss is *strongly* nonspherical, e.g., restricted to an equatorial disk or to polar jets.) Space telescopes will presumably be adequate for high-resolution imaging, but special ground-based visual wavelength imaging, under superb atmospheric conditions and enhanced by computer processing, may also be useful and interesting.

#### V. SUMMARY

In this paper we have noted several important points: (1) The 15-year-old temperature estimate for the opaque surface associated with  $\eta$  Car,  $T \approx 30,000$  K (Davidson 1971), is not yet altered by newer data. A variety of continuum and emission-line observations during the years 1965–1982 make it difficult to see how this temperature can be much less than 25,000 K. We believe that temperatures much hotter than 35,000 K are also unlikely in light of the same data. These estimates refer to the opaque surface, which may be cooler than the surface of the star itself. (2) The same temperature estimate and, independently, the infrared continuum both imply that either the presently observed mass loss rate of  $\eta$  Car is less than  $\sim 10^{-2.4} M_{\odot} \text{ yr}^{-1}$  (very likely less than  $10^{-3} M_{\odot} \text{ yr}^{-1}$ ), or else the mass outflow is confined to a narrow range of directions. Most of the star’s mass loss observed during the past 200 yr may have occurred between 1830 and 1850. (3) In the ejecta, specifically in the S condensation, most of the CNO is indeed nitrogen, as we asserted earlier (Davidson, Walborn, and Gull 1982). However, because the results depend on ionization and thermal structure, which require theoretical modeling, and because some oxygen and carbon may be in solid grains, we find it difficult to derive precise C/N/O abundance ratios. The gaseous silicon abundance is of indirect interest in this connection. (4) We find a helium mass fraction  $Y \approx 0.40 \pm 0.03$  in the S condensation and, by implication, in the star’s outer layers. This appears to indicate that the star is in a moderately—but not extremely—late stage of evolution. (5) There are some unexplained discrepancies in the S condensation’s emission line ratios, as well as poorly understood continuum emission.

These points are *results* of our observations, but we hesitate to call them *conclusions*. Aside from imperfections in the data, we have no appropriate, detailed theoretical models for comparison. At least two types of model would be highly useful. First, we need calculations of emergent spectra from very low gravity, CNO-processed stellar atmospheres with dense winds; these could be used especially to analyze the 1200–2000 Å “core” spectrum of  $\eta$  Car. There would be four obvious goals: to check the validity of our circa 30,000 K temperature estimate, to decide whether or not the visible surface is the stellar surface, to estimate the mass loss rate in the stellar wind, and to understand the sporadic instability of the star’s surface.

A second type of model that we need concerns the S condensation. Because conditions in the homunculus are very complicated, the outer condensations (among which S is brightest) offer our best hope of determining the chemical composition of  $\eta$  Car. And, as noted in § III above, self-consistent calculations of position-dependent ionization and thermal structure are needed for analyzing the spectrum of S. Such calculations would refine our abundance estimates and would also help us to understand the strong ultraviolet continuum and the emission line “discrepancies” mentioned in § III. One simplifying feature of the S condensation is that its dynamics, heating, and cooling involve essentially only three elements, hydrogen, helium, and nitrogen, and among these we already know the hydrogen/helium abundance ratio to useful accuracy. This object is worthy of consideration by researchers who have developed appropriate computer programs to deal with astrophysical shocks.

Other theoretical calculations are also desirable, notably including improved models of interior evolution in a star like  $\eta$  Car (cf. Maeder 1983) and, if possible, models of ionization and heating in the homunculus.

New observations of  $\eta$  Car are definitely worthwhile; there are major gaps in the data even though this is such a bright and unique object. Modern spectrophotometry of the entire homunculus—updated and improved observations in the same vein as those by Rodgers and Searle (1967)—are needed for several purposes, including an estimate of how much the circumstellar reddening has changed since the 1960s (cf. Pagel 1969a; Davidson 1971; § IV) and whether this can explain the star’s gradual increase in apparent brightness. Spectrophotometry of just the core would also be interesting.

The apparent brightness of the entire object should be monitored by continuum photometry using interference filters, not just *UBV* photometry, which is seriously perturbed by emission lines. The brightness of the core, relative to the entire homunculus, is relevant but poorly known (Davidson and Ruiz 1975).

In §§ II and III we have explained why better ground-based spectrophotometry would be useful: our data are somewhat ambiguous regarding spatial coverage. Spectroscopy of other condensations, within the homunculus as well as outside it, would also be worthwhile. (We note in passing that the “jet” on the northeast side of the homunculus, pointing toward the NN condensation [see Figs. 1 and 2], has a stronger visual wavelength continuum than the outer condensations. Probably it contains a larger concentration of dust; but why?)

Desirable Space Telescope observations of  $\eta$  Car are so obvious that we need not discuss them; imaging at high spatial resolution, at visual as well as ultraviolet wavelengths, may be as interesting as improved ultraviolet spectrophotometry. One particular question that should be answered as soon as pos-

sible, because it strongly affects our interpretation of the nature of the object, is whether  $\eta$  Car is a binary system.

Finally, we append to this paper an odd but possibly significant historical note. Because  $\eta$  Car is surrounded by shells of "old" ejecta (see Walborn, Blanco, and Thackeray 1978 and references therein), and considering its general nature, we suspect that bright eruptions of this star, such as the 19th-century outburst, may recur at intervals of several hundred years. Indeed it would be useful to know whether this suspicion is true. The star is so far south that such events would have gone unrecorded before the 16th century—*except* that, because of precession, in ancient times  $\eta$  Car was not so far south. Around 2500 years ago, for instance, its declination was  $-47^\circ 6'$ , similar to the present-day declination of the southern edge of Scorpius. Then it could have been seen by many of the astronomical observers of that time, above their southern horizons during spring evenings or winter mornings. During the major 19th century event,  $\eta$  Car was a 1st mag star for several years—far longer in duration than a supernova. Thus, if similar eruptions occurred between 2000 and 5000 yr ago, some experienced observers would have seen them.

An amazingly relevant conjecture was stated nearly a

century ago by Peter Jensen (1890), who noted various stars or constellations associated with the Sumerian god Ea. (Astronomers may recall Ea's implausible but entertaining appearance in Shklovskii and Sagan 1966.) One particular far southern star associated with Ea was said to be conspicuously variable, leading Jensen to identify it with  $\eta$  Car! However, we are warned by R. van Gent (private communication) that other stars were also characterized as variable, and since Jensen's time other authors have proposed alternative identifications of the Ea star. Therefore Jensen's conjecture is very uncertain, and the question of  $\eta$  Car in ancient times remains tantalizing as well as astrophysically significant.

We are grateful to R. M. Humphreys, H. J. G. L. M. Lamers, and T. J. Jones for valuable discussions about stars like  $\eta$  Car; to R. P. Stone for kindly providing data on a calibration star mentioned in § II; to J. N. Heckathorn for producing Figure 4; to A. Aaboe and especially to R. van Gent for skeptical comments regarding Jensen's conjecture; to the IUE support staff for valuable assistance in data reduction; and to D. A. Allen for useful comments on the original version.

## REFERENCES

- Ade, P., and Pagel, B. E. J. 1969, *Observatory*, **90**, 6.  
 Aitken, D. K., Jones, B., Bregman, J. D., Lester, D. F., and Rank, D. M. 1977, *Ap. J.*, **217**, 103.  
 Allen, D. A. 1979, *M.N.R.A.S.*, **189**, 1P.  
 Allen, D. A., Jones, T. J., and Hyland, A. R. 1985, *Ap. J.*, **291**, 280.  
 Andriess, C. D., Donn, B. D., and Viotti, R. 1978, *M.N.R.A.S.*, **185**, 771.  
 Andriess, C. D., Packet, W., and de Loore, C. 1981, *Astr. Ap.*, **95**, 202.  
 Appenzeller, I. 1970, *Astr. Ap.*, **5**, 355.  
 Bath, G. T. 1979, *Nature*, **282**, 274.  
 Brugel, E. W., Shull, J. M., and Seab, C. G. 1982, *Ap. J. (Letters)*, **262**, L35.  
 Cassatella, A., Giangrande, A., and Viotti, R. 1979, *Astr. Ap.*, **71**, L9.  
 Chlebowski, T., Seward, F. D., Swank, J., and Szymkowiak, A. 1984, *Ap. J.*, **281**, 665.  
 Davidson, K. 1971, *M.N.R.A.S.*, **154**, 415.  
 Davidson, K., Dufour, R. J., Walborn, N. R., and Gull, T. R. 1984, in *IAU Symposium 105, Observational Tests of Stellar Evolution Theory*, ed. A. Maeder and A. Renzini (Dordrecht: Reidel), p. 261.  
 Davidson, K., and Netzer, H. 1979, *Rev. Mod. Phys.*, **51**, 715.  
 Davidson, K., and Ruiz, M. T. 1975, *Ap. J.*, **202**, 421.  
 Davidson, K., Walborn, N. R., and Gull, T. R. 1982, *Ap. J. (Letters)*, **254**, L47.  
 de Jager, C. 1980, *The Brightest Stars* (Dordrecht: Reidel).  
 ———. 1984, *Astr. Ap.*, **138**, 246.  
 Draine, B. T., and Lee, H. M. 1984, *Ap. J.*, **285**, 89.  
 Durrance, S. T., Feldman, P. D., and Weaver, H. W. 1983, *Ap. J. (Letters)*, **267**, L125.  
 Feinstein, A., Marraco, H. G., and Muzzio, J. C. 1973, *Astr. Ap. Suppl.*, **12**, 331.  
 Forte, J. C. 1978, *A.J.*, **83**, 1199.  
 Gehrz, R. D., Ney, E. P., Becklin, E. E., and Neugebauer, G. 1973, *Ap. Letters*, **13**, 89.  
 Giles, K. 1977, *M.N.R.A.S.*, **180**, 57P.  
 Harvey, P. M., Hoffman, W. F., and Campbell, M. F. 1978, *Astr. Ap.*, **70**, 165.  
 Ho, Y. K., and Henry, R. J. W. 1984, *Ap. J.*, **284**, 435.  
 Humphreys, R. M., and Davidson, K. 1979, *Ap. J.*, **232**, 409.  
 ———. 1984, *Science*, **223**, 243.  
 Hyland, A. R., Robinson, G., Mitchell, R. M., Thomas, J. A., and Becklin, E. E. 1979, *Ap. J.*, **233**, 145.  
 Jensen, P. C. A. 1890, *Die Kosmologie der Babylonier* (Strassburg: Trübner), pp. 24–28.  
 Lambert, D. L. 1969, *Nature*, **223**, 726.  
 Lamers, H. J. G. L. M. 1985, *Astr. Ap.*, in press.  
 MacAlpine, G. M., Davidson, K., Gull, T. R., and Wu, C.-C. 1985, *Ap. J.*, **294**, 147.  
 Maeder, A. 1983, *Astr. Ap.*, **120**, 113.  
 Melnick, J., Ruiz, M. T., and Maza, J. 1982, *Astr. Ap.*, **111**, 375.  
 Mendoza, C. 1983, in *IAU Symposium 103, Planetary Nebulae*, ed. D. R. Flower (Dordrecht: Reidel), p. 143.  
 Mendoza, C., and Zeppen, C. J. 1982, *M.N.R.A.S.*, **198**, 127.  
 Mitchell, R. M., Robinson, G., Hyland, A. R., and Jones, T. J. 1983, *Ap. J.*, **271**, 133.  
 Moos, M. W., Durrance, S. T., Skinner, T. E., Feldman, P. D., Bertaux, J.-L., and Festou, M. C. 1983, *Ap. J. (Letters)*, **275**, L19.  
 Mundt, R., and Witt, A. N. 1983, *Ap. J. (Letters)*, **270**, L59.  
 Nussbaumer, H., and Rusca, C. 1979, *Astr. Ap.*, **72**, 129.  
 Nussbaumer, H., and Storey, P. J. 1982, *Astr. Ap.*, **109**, 271.  
 Osterbrock, D. E., and Wallace, R. K. 1977, *Ap. Letters*, **19**, 11.  
 Pagel, B. E. J. 1969a, *Nature*, **221**, 325.  
 ———. 1969b, *Ap. Letters*, **4**, 221.  
 Penston, M. V., et al., 1983, *M.N.R.A.S.*, **202**, 833.  
 Pottasch, S. R., Wesselius, P. R., and van Duinen, R. J. 1976, *Astr. Ap.*, **47**, 443.  
 Pradhan, A. K. 1978, *M.N.R.A.S.*, **183**, 89P.  
 Rodgers, A. W., and Searle, L. 1967, *M.N.R.A.S.*, **135**, 99.  
 Seaton, M. J. 1975, *M.N.R.A.S.*, **170**, 475.  
 ———. 1978, *M.N.R.A.S.*, **185**, 5P.  
 Shklovskii, I. S., and Sagan, C. 1966, *Intelligent Life in the Universe* (San Francisco: Holden-Day), pp. 456–461.  
 Thé, P. S., Bakker, R., and Antalova, A. 1980, *Astr. Ap. Suppl.*, **41**, 93.  
 Thé, P. S., Tjin A Djie, H. R. E., Kudritzki, R. P., and Wesselius, P. R., 1980, *Astr. Ap.*, **91**, 360.  
 Thomas, J. A., Robinson, G., and Hyland, A. R. 1976, *M.N.R.A.S.*, **174**, 711.  
 van Genderen, A. M., and Thé, P. S. 1985, *Space Sci. Rev.*, **39**, 317.  
 Viotti, R. 1969, *Ap. Space Sci.*, **5**, 323.  
 Viotti, R., Giangrande, A., Cassatella, A., and Macchetto, F. 1981, *Space Sci. Rev.*, **30**, 235.  
 Walborn, N. R. 1971, *Ap. J. (Letters)*, **167**, L31.  
 ———. 1973, *Ap. J.*, **179**, 517.  
 ———. 1976, *Ap. J. (Letters)*, **204**, L17.  
 Walborn, N. R., Blanco, B. M., and Thackeray, A. D. 1978, *Ap. J.*, **219**, 498.  
 Walborn, N. R., and Hesser, J. E. 1975, *Ap. J.*, **199**, 535.  
 Walborn, N. R., and Liller, M. 1977, *Ap. J.*, **211**, 181.  
 Westphal, J. A., and Neugebauer, G. 1969, *Ap. J. (Letters)*, **156**, L45.  
 Whitelock, P. A., Feast, M. W., Carter, B. S., Roberts, G., and Glass, I. S. 1983, *M.N.R.A.S.*, **203**, 385.  
 Zanella, R., Wolf, B., and Stahl, O. 1984, *Astr. Ap.*, **137**, 79.

KRIS DAVIDSON: Astronomy Dept., University of Minnesota, 116 Church St. S.E., Minneapolis, MN 55455

REGINALD J. DUFOUR: Dept. of Space Physics and Astronomy, 204K Space Sci. Bldg., Rice University, Houston, TX 77001

THEODORE R. GULL: Code 680, NASA/Goddard Space Flight Center, Greenbelt, MD 20771

NOLAN R. WALBORN: Space Telescope Science Institute, Homewood Campus, Baltimore, MD 21218